Chemical speciation of trace metals in atmospheric deposition and impacts on soil geochemistry and vegetable bioaccumulation near a large copper smelter in China

Hailong Liu[1], Jun Zhou[2], Min Li[1], Daniel Obrist[3], Xiao-Zhi Wang[1], and Jing Zhou[2]

[1]College of Environmental Science and Engineering, Yangzhou University
[2]Institute of Soil Science, Chinese Academy of Sciences
[3]Department of Environmental, Earth, and Atmospheric Sciences, University of Massachusetts

November 26, 2022

Abstract

Atmospheric deposition is an important source of trace metals to surface environments, but knowledge about plant bioavailability of recently deposited metals is limited. We performed a fully factorial soil and atmosphere exposure experiment with three vegetables (radish, lettuce, and soybean), which allowed to effectively distinguish impacts of recently deposited metals (<1 year) from longer-term metal exposures in soils. Results showed that recently deposited Cu, Cd, and Pb accounted for 0.5-15.2% of total soil Cu, Cd, and Pb pools near emission source, while they contributed 15-76% of Cu, Cd, and Pb concentrations in edible parts of vegetables. The soil retention of recently deposited metals (52-73%) presented as higher mobile fractions than these previously present in soils (7-42%). These findings highlight a preferential uptake and high rates of bioaccumulation of deposited metals in vegetables and implicated that quick and potentially stronger reduction can be achieved by reducing current atmospheric source loads.

Chemical speciation of trace metals in atmospheric deposition and impacts on soil geochemistry and vegetable bioaccumulation near a large copper smelter in China

Hai-Long Liu [a, b] Jun Zhou [a, c, d,] *, Min Li [b], Daniel Obrist [c], Xiao-Zhi Wang [b], Jing Zhou [a, d,] *

a. Key Laboratory of Soil Environment and Pollution Remediation, Institute of Soil Science, Chinese Academy of Sciences, Nanjing 210008, P.R. China

b. College of Environmental Science and Engineering, Yangzhou University, Yangzhou 225000, P.R. China

c. Department of Environmental, Earth and Atmospheric Sciences, University of Massachusetts, Lowell, MA 01854, USA

d. National Engineering and Technology Research Center for Red Soil Improvement, Red Soil Ecological Experiment Station, Chinese Academy of Sciences, Yingtan 335211, P.R. China

*Corresponding author: zhoujun@issas.ac.cn (Jun Zhou) and zhoujing@issas.ac.cn (Jing Zhou).

Add: 71st East Beijing Road, Nanjing, China, 210008.

Key Points

- Bioavailable fractions of trace metals from recent atmospheric deposition were higher compared to metals originally present in soils.
- Recently deposited trace metals contributed 15-76% of cupper, cadmium and lead to edible parts of vegetables.
- Reducing current atmospheric deposition loads of trace metals has quick and strong effects on their accumulation in the vegetable.

Abstract: Atmospheric deposition is an important source of trace metals to surface environments, but knowledge about plant bioavailability of recently deposited metals is limited. We performed a fully factorial soil and atmosphere exposure experiment with three vegetables (radish, lettuce, and soybean), which allowed to effectively distinguish impacts of recently deposited metals (<1 year) from longer-term metal exposures in soils. Results showed that recently deposited Cu, Cd, and Pb accounted for 0.5-15.2% of total soil Cu, Cd, and Pb pools near emission source, while they contributed 15-76% of Cu, Cd, and Pb concentrations in edible parts of vegetables. The soil retention of recently deposited metals (52-73%) presented as higher mobile fractions than these previously present in soils (7-42%). These findings highlight a preferential uptake and high rates of bioaccumulation of deposited metals in vegetables and implicated that quick and potentially stronger reduction can be achieved by reducing current atmospheric source loads.

Keywords: Wet and dry deposition; Metal speciation; Soil geochemistry; Vegetable bioaccumulation

Plain Language Summary

Atmospheric deposition is a globally important source of trace metals in agricultural soils but limited attention has been given to the risk of recently deposited metals for bioaccumulation in vegetables. We performed a fully factorial soil and atmosphere exposure experiment with vegetables (radish, lettuce, and soybean) planted across three sites located along a strong gradient of atmospheric deposition, which allowed to distinguish between impacts of recently deposited metals and metals originally present in soils. The results demonstrated that recently deposited trace metals showed high bioavailability contributing preferentially to uptake in edible parts of vegetables compared to metals previously present in soils. These findings highlight a key role of atmospheric deposition for trace metals in bioaccumulation in vegetables and suggest effective measures for reducing atmospheric emissions of trace metals should been implemented to reduce environmental risks of food contamination.

1. Introduction

Soil pollution of farmland in China has caused extensive concerns in the last decades due to adverse impacts on ecosystems and human health (Hu et al., 2016; Zhao et al., 2015). A key survey by the Ministry of Ecology and Protection of the People's Republic of China conducted between 2005 and 2013 indicated that 19.4% of collected samples of agricultural soils exceeded the environmental quality standard of China, especially by exceedance of trace metals loads (cadmium, copper, lead, arsenic, mercury, chromium, etc.) causing heavy pollution. According to estimates, more than 12×10^{6} t of annual crop production in China is polluted by trace metals potentially causing health risks via dietary intake, while direct inhalation and dermal contact may be of lower concern (Hu et al., 2016; Zhang et al., 2019). Identification of the sources and impacts of trace metals in agricultural systems is a first and critical step to protect agricultural production safety (Imseng et al., 2018; Salmanzadeh et al., 2017). Principle external sources of trace metals in farmland of China include agricultural irrigation, pesticide and fertilizer application, and atmospheric deposition (Ha et al., 2014; Larson, 2014; Peng et al., 2019). Previous studies were focused largely on pollution via the former two sources (Habibollahi et al., 2018; Wang et al., 2018), while effects of atmospheric deposition are less known. Atmospheric emissions of trace metals from anthropogenic activities have rapidly increased in the last decades and emissions of Cd, Cu, Pb, As, and Zn from anthropogenic sources into the atmosphere in China have reached 530 tons (Cd), 9,500 tons (Cu), 14,000 tons (Pb), 2,500 tons (As), and 22,000 tons (Zn) in 2012, respectively (Tian et al., 2015). Atmospheric deposition has been an important pathway for the transfer trace metals from point source of atmospheric emissions to surface environments (Bridgestock et al., 2017; Chien et al., 2019; Chrastny et al., 2015) and are estimated to account for more than 50% of total As, Cd, Cr, Hg, and Pb loads in agricultural soils across China (Peng et al., 2019).

Atmospheric deposition is considered to have high bioavailability in surface environments (Wang et al., 2017; Wilcke & Kaupenjohann, 1998). Research indicated that 68-74% of Cd and Zn in wet deposition are in dissolved fractions and that 25-33% of Cd and Zn in dry deposition occur in water-soluble fractions (Morselli et al., 2003). Other studies also indicated that trace metals from atmospheric deposition have high proportion of bioavailable fractions (Prieto-Parra et al., 2017; Pyeong-Koo et al., 2015) as they are preferentially retained in surface soil aggregates and found to have higher exchangeable fractions compared to metals originally present in soil aggregates (Wilcke & Kaupenjohann, 1998). Another study suggested atmospheric Cu deposition show high toxicity and inhibit phytoplankton growth in the Mediterranean Sea (Jordi et al., 2012). Combined, these studies suggest that trace metals recently deposited (<1 year of deposition) may have particularly high environmental risks and potentially high uptake and biological effects in vegetables. Differentiation of effects of recently deposited (e.g., during vegetable growing period) and original metal loads in soils available to vegetables is crucial to understand how metals accumulation may respond to changing metal deposition loads (Hintelmann et al., 2002).

Here, we present the results of a systematic experiment on bioaccumulation of trace metals from recent atmospheric deposition versus longer-term soil exposures in three vegetables (radish, lettuce, and soybean) by means of a fully factorial soil and atmosphere exposure design including seven treatment groups (2 to 3 soil exposures (S1, S2, and S3 soils) and 3 atmospheric exposures (A1, A2, and A3 sites)) conducted near a copper smelter of Guixi city, known as China's copper capital located in southeastern China (Supplementary information, Fig. S1 and Table S1). The study includes detailed analysis of soil and atmospheric deposition including chemical speciation and bioavailability estimates of trace metals.

2. Materials and methods

2.1. Experimental design

To constrain bioavailability of recently deposited trace metals in soil-vegetable system, a fully factorial soil and atmosphere exposure design with replications (n = 3) in soil profile (dimensions: 0.58 m length×0.44 m wide×0.32 m height) was conducted between July 2017 and June 2018 including seven treatment groups (Fig. S2 and Table S2). Moderately (80.02±0.88 mg/kg Cu, 0.72±0.05 mg/kg Cd, and 50.20±0.43 mg/kg Pb) and heavily (556.67±12.61 mg/kg Cu, 1.66±0.05 mg/kg Cd, and 74.13±1.77 mg/kg Pb) polluted soils (due to the long-term metal smelting emissions) from two sites (A2 and A3) were transferred to the remote site A1, while unpolluted soil (23.32±0.09 mg/kg Cu, 0.22±0.01 mg/kg Cd, and 29.61±0.19 mg/kg Pb) from site A1 was transferred to polluted sites A2 and A3. As a result, three treatment groups were placed at the control site A1, including A1-S1 (filled with soil from the control site), A1-S2 (filled with soil from the moderate deposition site A2), and A1-S3 (filled with soil from the high deposition site A3). Two treatment groups were placed at the moderate deposition site A2, including A2-S1 (filled with the soil from the control site) and A2-S2 (filled with the soil from moderate deposition site). Finally, two treatment groups were placed at the high deposition site A3, including A3-S1 (filled with the soil from the control site) and A3-S3 (filled with the soil from high deposition site). To manage the high number of treatment numbers, we selected not to expose soil from moderate deposition site A2 at the high atmospheric deposition site A3, and vice versa not to expose soil from the high deposition site A3 at the moderate atmospheric deposition site A2.

Three widely cultivated vegetables, including radish (*Raphanus sativus* L., rhizome vegetable), lettuce (*Lactuca sativa* L., leaf vegetable) and soybean (*Phaseolus vulgaris* L., fruit vegetable), were grown in each of these soil-atmosphere exposure treatments, resulting in a total of 63 plant samples (2-3 soil exposures, 3 atmospheric exposures, 3 vegetable types, 3 replications). The vegetable types were chosen because they represented different edible parts for human consumption, i.e., rhizomes for radish, leaves for lettuce, and seeds for soybean. The planting order and growing season of three vegetables were chosen according to local farming practices and described in Supplementary information (SI).

The treatment A1-S1 (soil from the control site and exposed to low atmospheric deposition) was used to estimate bioaccumulation under background conditions. The sequence of treatments A1-S1, A1-S2, and A1-S3 representing increasing soil trace metals exposed to low atmospheric deposition allowed to quantify effects of past (i.e., >1 year) atmospheric deposition impacts (Zhou et al., 2018). Differences among treatments A1-S1, A2-S1, and A3-S1 were used to quantify increasing atmospheric deposition loads of trace metals in low background soils. Finally, treatments A1-S2 and A2-S2 and treatments A1-S3 and A3-S3 were similarly designed to assess increasing atmospheric deposition effects in moderately and heavily polluted soils. Further details on the experimental design are described in SI.

2.2. Sample collection and analysis

2.2.1. Atmospheric deposition measurements and characterization of trace metal deposition chemistry, speciation, and size distribution

Atmospheric wet and dry deposition samples were collected monthly from July 2017 to June 2018 at each site using automatic wet and dry deposition sampler (APS-3A, Changsha Xianglan Scientific Instruments Co., Hunan, China). In wet deposition, hydrodynamic diameter, pH, and size distribution (> 0.45 μm for particulate, < 0.45 μm for dissolved fraction, and < 3 kDa for defined ionic fraction) of Cu, Cd, and Pb were determined (Javed et al., 2017). For dry deposition, mineral composition by X-ray diffractometer (XRD, Ultima IV, Japan) analysis and chemical fractions of Cu, Cd, and Pb (F1 exchangeable, F2 carbonate, F3 reducible, F4 organic and sulfide, and F5 residual fractions) by Tessier five-step sequential extraction were determined. In addition, the mineral composition of dust samples collected from a smelter bag filter in the Guixi copper smelter was also characterized by XRD to confirm that the likely origin of dry deposition is linked to this emission source. Further details on the samplers and sampling and analytical methods are detailed in SI.

2.2.2. Vegetable and soil sampling and trace metal characterization

Three vegetables (radish, lettuce, and soybean) were grown in sequence for the duration of 60, 45, and 75 days, respectively and harvested in early March, mid-April, and late June 2018, respectively. Contents of Cu, Cd, and Pb in vegetable tissues (rhizomes (or root) and shoot for radish and lettuce, root, stem, leaf, pod, and seed for soybean) were extracted using a 1:1 mixture of HNO_3 and H_2O_2. Surface soils were collected after final harvest in June 2018 by stratified sampling in the following depth increments: 0-2, 2-4, 4-6, 6-10, 10-15, and 15-20 cm. Concentration and speciation of Cu, Cd, and Pb in soils were characterized by Tessier five-step sequential extraction. Detailed description of sampling and analytical methods can be found in SI.

2.2.3. Bioaccumulation contribution factors

Contributions (C, %) of trace metals originally present in soils to vegetable bioaccumulation were estimated as follows:

$$C = (MC_{A1\text{-}S2} - MC_{A1\text{-}S1})/(MC_{A1\text{-}S2})$$

$$C = (MC_{A1\text{-}S3} - MC_{A1\text{-}S1})/(MC_{A1\text{-}S3}) \qquad (1)$$

where $MC_{A1\text{-}S2}$, $MC_{A1\text{-}S3}$, and $MC_{A1\text{-}S1}$ are concentrations of Cu, Cd, and Pb (mg/kg dry weight) in vegetable tissues grown in the moderate pollution soil (S2), heavy pollution soil (S3), and background soil (S1) respectively using samples placed at the control site (A1).

Contributions (C, %) of recently deposited trace metals to vegetable bioaccumulation were estimated as follows:

$$C = (MC_{A2\text{-}S1} - MC_{A1\text{-}S1})/(MC_{A2\text{-}S1})$$

$$C = (MC_{A3\text{-}S1} - MC_{A1\text{-}S1})/(MC_{A3\text{-}S1})$$

$$C = (MC_{A2\text{-}S2} - MC_{A1\text{-}S2})/(MC_{A2\text{-}S2})$$

$$C = (MC_{A3\text{-}S3} - MC_{A1\text{-}S3})/(MC_{A3\text{-}S3}) \qquad (2)$$

where $MC_{A2\text{-}S1}$, $MC_{A2\text{-}S2}$, $MC_{A1\text{-}S1}$, and $MC_{A1\text{-}S2}$ are concentrations of Cu, Cd, and Pb (mg/kg dry weight) in vegetable tissues in moderate deposition site (A2) and control site (A1) filled with the soils S1 and S2, and $MC_{A3\text{-}S1}$, $MC_{A3\text{-}S3}$, $MC_{A1\text{-}S1}$, and $MC_{A1\text{-}S3}$ represent exposures to high deposition (A3) and control (A1) sites filled with soils S1 and S3.

2.3. Statistical Analysis

Statistical analyses for all data were performed using SPSS 20.0. The differences of Cu, Cd, and Pb concentrations in soils and vegetables were analyzed among A1, A2, and A3 sites based on the one-way analysis of variance (ANOVA, Least Significant Difference test). All differences in means (n = 3) were considered significant at the $p = 0.05$ level (two-tailed).

3. Result and discussion

3.1 Cu, Cd, and Pb accumulation in vegetable and nutritional quality analysis

Cu, Cd, and Pb concentrations in soybean seed, the edible part of that vegetable, grown in control soils were 20.21±0.99, 0.38±0.02, and 0.32±0.01 mg/kg when exposed to high atmospheric deposition (A3-S1) and significantly higher ($p < 0.05$) compared to low atmospheric exposures (A1-S1: 15.41±1.14, 0.26±0.01, and 0.18±0.01 mg/kg) (Fig. 1). Similarly, Cu, Cd, and Pb concentrations in radish rhizomes (the edible part) grown in control soils (A1-S1) of 3.97±0.25, 0.52±0.03, and 0.38±0.01 mg/kg were significantly increased under high atmospheric deposition (A3-S1, 7.36±0.38, 1.21±0.12, and 0.83±0.03 mg/kg) (Fig. S3). For lettuce, Cu, Cd, and Pb concentrations of shoots grown in control soils (A1-S1, 8.15±0.40, 3.78±0.28, and 1.37±0.03 mg/kg) significantly increased to 33.96±1.96, 8.25±0.26, and 3.75±0.11 mg/kg (A3-S1) when exposed to high atmospheric deposition (Fig. S4). Meanwhile, trace metals concentrations of other, non-edible root and shoot tissues of the three vegetables grown in control and strongly polluted soils exposed to the high deposition (A3) were also statistically significantly increased compared to those exposed at the control site (A1) (Fig. 1, Fig. S3, and Fig. S4). Similarly, plant Cu, Cd, and Pb concentrations in control and moderately polluted soils were significantly and slightly increased when exposed to moderate deposition (A2) compared to the control site (A1) (Fig. 1, Fig. S3, and Fig. S4). For instance, Cu, Cd, and Pb concentrations of lettuce shoot in moderately polluted soil exposed to moderate deposition (A2) were 19.75±0.65, 16.92±0.57, and 3.43±0.12 mg/kg (A2-S2), which were significantly higher compared to low atmospheric exposures (A1-S2: 15.76±0.91, 14.66±0.44, and 2.81±0.09 mg/kg), respectively (Fig. S4). These results showed that trace metals accumulation in vegetable plant are significantly and slightly increased under both high and moderate atmospheric deposition loads.

Trace metals concentrations of vegetable plants strongly responded to longer-term soil pollution levels (S1, S2, and S3) as well. For instance, Cu, Cd, and Pb concentrations of soybean seeds from control soils (A1-S1: 15.41±1.14, 0.26±0.01, and 0.18±0.01 mg/kg) significantly increased to 19.06±1.03, 0.68±0.02, and 0.25±0.01 mg/kg in moderately polluted soil (A1-S2) and 24.36±2.18, 0.99±0.02, and 0.29±0.01 mg/kg in heavily polluted soil (A1-S3) (Fig. 1). Similarly, trace metals concentrations of other tissues in the three vegetables grown in polluted soils (S2 and S3) also were statistically significantly increased ($p < 0.05$) compared to those in control soil (S1) (Fig. 1, Fig. S3, and Fig. S4). Different soil exposures S1 through S3 are indicative of effect of past (i.e., >1 year) atmospheric deposition impacts similar to observed increases in previous studies for Pb in vegetables and maize from long-term atmospheric deposition inputs near nonferrous metal smelters (Bi et al., 2009; Li et al., 2012).

By comparing concentration increase in tissues of moderate and high atmospheric exposures compared to control locations, we calculated the percentage contribution of recently (<1 year) atmospheric deposition according to the Eq. (2). Contributions induced by atmospheric deposition to Cu, Cd, and Pb in soybean seed ranged from 2-14% and 15-42% in plants exposed to moderate (A2) and high (A3) atmospheric deposition sites, respectively (Table S3). For radish, Cu, Cd, and Pb from atmospheric deposition in rhizomes, representing the edible part, ranged from 5-12% and 16-57% under moderate and high atmospheric deposition exposure sites, respectively (Table S4). For lettuce, Cu, Cd, and Pb from atmospheric deposition in shoots as the edible parts ranged from 13-35% and 18-76% under moderate and high atmospheric deposition exposure sites, respectively (Table S5). Similarly, by comparing concentration increases in tissues due to soil exposures at the control site, we calculated the percentage contribution of earlier (i.e., >1 year) atmospheric deposition to trace metals concentrations according to the Eq. (1). Contributions by soil exposures to Cu, Cd, and Pb in soybean seed ranged from 19-62% and 29-74% in plants exposed to moderately (S2) and heavily (S3) polluted soils, respectively (Table S6). Similar results were also observed in radish rhizome and lettuce shoot (Table S6). These results indicate that trace metal accumulation in various vegetables and tissues exposed to recent atmospheric deposition was enhanced compared to original root-to-shoot transfer of trace metals from soils.

We also observed that contributions under high atmospheric deposition loads (A3-S1) were always higher in lettuce shoots compared to that of soybean seeds and radish rhizomes. For example, Cu contributions from recent deposition averaged 76% in lettuce shoots compared to 24% in soybean seeds and 46% in radish rhizomes. Similar effects were observed for Pb and Cd (Table S3, S4, and S5). These patterns may be related to different transfer pathways of trace metals to various tissues (Shahid et al., 2016): for example, atmospheric deposition can be absorbed by direct foliar uptake or indirectly through soil-root uptake after deposition (Schreck et al., 2014). Still, we propose that trace metals in radish rhizomes largely accumulate from soil-root transfer pathway, similar to a previous study that concluded that < 1% of foliar uptake can be translocated to root tissues (Shahid et al., 2016). For lettuce shoot and soybean seeds, the two uptake pathways may occur simultaneously. Indeed, significant differences in Cu, Cd and Pb concentrations were observed between washed and unwashed leaves and pods of soybean (see description of experimental design in Text S5) suggesting that airborne trace metals can be directly taken up and fixed in leaves and pods (Fig. 1) and then be partially transported from the leaves to seeds via phloem stream along with photosynthates (Shahid et al., 2016). Higher trace metals concentrations of lettuce and soybean roots exposed at high deposition site also indicate a pathway of atmosphere-soil-root transfer similar to that in radish rhizome whereby metals in root are transported to the aerial parts via xylem transport. Unfortunately, the present study cannot accurately distinguish the effect of the two transfer pathways because pathways likely occur simultaneously.

It is noteworthy that recently deposited Cu, Cd, and Pb at the high deposition site (A3-S1) accounted for 1-15% of total trace metal pools in soils but 24-76% in edible vegetation parts. In heavily polluted soils (A3-S3), recent deposition accounted for soil pool sizes of 0.5-2.1% while in edible plants recent atmospheric deposition accounted for 15-54% of loads. While recently deposited metals contributed much lower proportions (< 1%) to soils under moderate deposition in treatments A2-S1 and A2-S2, contribution to edible plants from recent deposition were between 2 and 35%. These results highlight a high bioaccumulation potential of recently deposited trace metals in vegetables roots, leaves, and seeds. This is an important finding and reasons for high bioaccumulation are discussed in sections 3.2 and 3.3.

3.2 Cu, Cd, and Pb in soils

Total Cu and Cd concentrations in surface horizons (0-2 or 2-4 and 4-6 cm) exposed at deposition sites A2 and A3 after one year were significantly increased compared to corresponding soils exposed at the control site A1 (Fig. 2A-F). Similarly, Pb concentrations in topsoil (0-4 cm) exposed at sites A2 and A3 were slightly (but not statistically significant) increased compared to soil exposed at A1 (Fig. 2G-I). Obviously, original soil metal concentrations differed significantly between soils collected from the three sites (mean values of 0.22-1.66 mg/kg for Cd and 23.32-556.67 mg/kg for Cu, Table S1). Combined, soils showed statistically significant concentration differences in surface soil metal concentrations after one year from lowest to highest exposure sites, with a mean increase of mean 0.19 mg/kg for Cd and mean 34.73 mg/kg for Cu (Fig. 2 and Table S7). The results suggest that while farmland soils experience substantial long-term atmospheric deposition with highest pollution loads found nearby the large smelter, relatively short exposures (1 year) to high atmospheric deposition results in further trace metal concentration enhancements in surface soils. At the same time, total Cu, Cd, and Pb concentrations in deeper soils (6-20 cm profile) were not affected ($p > 0.05$) by different atmospheric deposition exposures (Fig. 2) indicating that recently deposited trace metals were largely retained in surface soil. Reason for efficient surface accumulation of trace metals include physical retention, adsorption and complexing effects from clay minerals, iron oxides and organic matter in the upper soil layers (Stolpe et al., 2013; Werkenthin et al., 2014).

Environmental risk of trace metals in soils strongly depended on chemical speciation, especially on exchangeable fractions (Liu et al., 2017; Uzu et al., 2009). Sequential extraction results in our study show that the concentrations and percentages of exchangeable Cu and Cd in the surface horizons exposed to moderate and high atmospheric deposition sites (A2 and A3) after one year were increased 110 to 610% (in concentrations) and 0.9 to 10.6 % (as percentage exchangeable, respectively; Table S7 and Fig. S5). For instance, exchangeable Cu and Cd (9.2±0.3 and 0.13±0.01 mg/kg) in the surface (0-2 cm profile) of background soils exposed to 1 year of high atmospheric deposition (A3-S1) was 6.1 and 2.2 times higher than exposed at the background site (A1-S1: 1.5±0.1 and 0.06±0.00 mg/kg). In addition, percentages of exchangeable fractions also increased, e.g., accounting for 17% and 29% for Cu and Cd at high atmospheric exposures in control soils (A3-S1, 0-2 cm profile) compared to background atmospheric exposures (A1-S1: 6% and 19%, respectively), under simultaneously decreased percentages of immobile Cu and Cd (Fig. S5). These results indicate that recently deposited trace metals in topsoil are present in highly bioavailable fractions exceeding availability of trace metals previously present in soils. This notion partly explains the finding of high bioaccumulation of recently deposited trace metals reported in vegetable in the section above (e.g. see Fig. 1).

3.3 Atmospheric Cu, Cd, and Pb deposition

Atmospheric deposition fluxes of Cu, Cd, and Pb, separated into wet and dry deposition components over the one year period of measurements (July 2017 to June 2018) at the three gradient sites (A1, A2, and A3) are shown in Fig. 3A. Deposition fluxes show strong gradients in deposition loads with distance from the smelter: highest annual bulk deposition (combined wet and dry deposition) of Cu, Cd, and Pb were 1091.8, 8.6, and 87.5 mg/m^2 in A3, which was about 9, 4, and 3 times higher than deposition measured at site A2 (117.2, 2.4, and 29.2 mg/m^2) and about 67, 9, and 13 times higher than at the control site A1 (16.4, 0.9, and 6.8 mg/m^2), respectively.

Chemical fractionation of wet deposition can reveal additional information about biological activities (Lee et al., 2015; Liu et al., 2017). Our results showed that most Cu, Cd, and Pb (85-97%) in wet deposition across the three study sites (Fig. 3B) was in dissolved and colloid fractions (< 0.45 μm). In addition, the ionic fraction (associated with < 3 kDa size particles) of Cu, Cd, and Pb accounted for 70-85% of total wet deposition. We propose that very low pH observed in wet deposition (3.07-6.30) (Table S8) promote particle dispersion and increases solubility of trace metals. Indeed, results of hydrodynamic diameter analysis (Table S8) showed that the main particles in wet deposition were in the nanometer scale (2.99-88.07 nm), which was consistent with or smaller than the previous report for metal particles sizes (50 nm -1 um) in cloud droplets (Li et al., 2013). The fractionation of trace metals in atmospheric deposition is important as metals in small size particles are more easily absorbed and bioaccumulated in crop (Ma et al., 2010; Peng et al., 2018).

We compared the mineralogical compositions of dry deposition across the three study sites with dust collected from the Cu smelter and found that they showed strong similarities. We show XRD fitting curves for site A3 and dust in Fig. 3D as an example. All samples were mainly composed of quartz, feldspar, calcite, and hydromica (Fig. 3D), suggesting that atmospheric deposition in the study area was related to emissions from the Cu smelter. Sequential extraction experiments of dry deposition (Fig. 3C) showed that Cu was primarily bound to organics and sulfides (Fraction F4: 57-71%) and in reducible fraction (F3: 13-22%), which is in agreement with the mineralogical composition of dust from the smelter and in deposition sample analysis that shows Cu sulfides and oxides (Cu_2S, Fe_5CuO_8, and Cu_2O) (Fig. 3D). Pb in dry deposition of the three study sites was dominantly bound to reducible fraction (fraction F3: 43-46%) and was followed by organics and sulfides (F4: 17-23%) (Fig.

3C). Additionally, a smaller fraction of Cu and Pb occurred in the exchangeable form (F1: Cu 8-10% and Pb 10-15%) indicating that dry deposited Cu and Pb in our study may be potentially less mobile. Compared to Cu and Pb, the exchangeable (F1) and carbonate fractions (F2) of Cd were highest (16-22% and 9-11%) indicating relatively high bioactivity of Cd (Liu et al., 2017). As mentioned, as the study area showed strong acid deposition and soils were strongly acidified (soil pH of 4.28-5.27) (Table S1), we suggest that the sum of a wet deposition (< 0.45 μm) plus dry deposition fractions F1 + F2 may serve as a measure of bioavailable fractions in our study. Following this approach, bioavailable fractions of Cu, Cd, and Pb from atmospheric deposition were in the range of 52-65% for Cu, 68-73% for Cd, and 53-58% for Pb of total deposition. Using the speciation in soils, the bioavailability of trace metals from measured atmospheric deposition exceeded the bioavailability in soils, which we determined to be 8-19% for Cu, 36-42% for Cd, and 7-14% for Pb (Table S7). The results indicate recently deposited trace metals to have much higher bioavailability compared to previous deposition or natural background of trace metals observed in soils. This notion further explains our finding: recently deposited trace metals have high bioavailability contributing preferentially to uptake in edible parts of vegetables compared to trace metals previously present in soils.

4 Environmental implications

Current remediation strategies of reducing trace metals in polluted cropland soils in China are mainly driven by immobilization of amendments in-situ, yet their effects are not particularly high (10%-50%) (Ali et al., 2020; Gong et al., 2020; Huang et al., 2020; Liu et al., 2020) and immobilization efficiencies decrease over time (Cui et al., 2016). The major implication of this study is that quick and potentially stronger reduction trace metal accumulation (2%-76%) in edible parts of vegetables can be achieved by reducing current atmospheric source loads. Therefore, eliminating and reducing current atmospheric deposition loads of trace metals should be considered as an environmental risk management strategy to reduce vegetable trace metal pollution.

Notes

The authors declare no competing financial interest.

Acknowledgements

This work was financially supported by the National Natural Science Foundation of China (41807385) and Key Scientific Research and Development Projects of Jiangxi Provence (20194ABC28010). We are also acknowledged Mei-Xiang Qiu, Qing-Cai Xu, and Man-Ju Zhu for the help in filed management in the three sites. Data will be made available at the website (https://www.researchgate.net/profile/Jun_Zhou43).

References

Ali, A., Shaheen, S.M., Guo, D., Li, Y., Xiao, R., Wahid, F., et al. (2020). Apricot shell- and apple tree-derived biochar affect the fractionation and bioavailability of Zn and Cd as well as the microbial activity in smelter contaminated soil, *Environmental Pollution*, *264*.

Bi, X., Feng, X., Yang, Y., Li, X., Shin, G.P.Y., Li, F., et al. (2009). Allocation and source attribution of lead and cadmium in maize (Zea mays L.) impacted by smelting emissions, *Environmental Pollution*, *157*(3), 834-839.

Bridgestock, L., Rehkamper, M., van de Flierdt, T., Murphy, K., Khondoker, R., Baker, A.R., et al. (2017). The Cd isotope composition of atmospheric aerosols from the Tropical Atlantic Ocean, *Geophysical Research Letters*, *44*(6), 2932-2940.

Chien, C., Benahabet, T., Torfstein, A., & Paytan, A. (2019). Contributions of Atmospheric Deposition to Pb Concentration and Isotopic Composition in Seawater and Particulate Matters in the Gulf of Aqaba, Red Sea, *Environmental Science & Technology*, *53*(11), 6162-6170.

Chrastny, V., Cadkova, E., Vanek, A., Teper, L., Cabala, J., & Komarek, M. (2015). Cadmium isotope fractionation within the soil profile complicates source identification in relation to Pb-Zn mining and smelting processes, *Chemical Geology*, *405*, 1-9.

Cui, H., Fan, Y., Xu, L., Zhou, J., Zhou, D., Mao, J., et al. (2016). Sustainability of in situ remediation of Cu- and Cd-contaminated soils with one-time application of amendments in Guixi, China, *Journal of Soils and Sediments*, *16*(5), 1498-1508.

Gong, L., Wang, J., Abbas, T., Zhang, Q., Cai, M., Tahir, M., et al. (2020). Immobilization of exchangeable Cd in soil using mixed amendment and its effect on soil microbial communities under paddy upland rotation system, *Chemosphere*, *262*, 127828-127828.

Ha, H., Olson, J.R., Bian, L., & Rogerson, P.A. (2014). Analysis of Heavy Metal Sources in Soil Using Kriging Interpolation on Principal Components, *Environmental Science & Technology*, *48*(9), 4999-5007.

Habibollahi, M.H., Karimyan, K., Arfaeinia, H., Mirzaei, N., Safari, Y., Akramipour, R., et al. (2018). Extraction and determination of heavy metals in soil and vegetables irrigated with treated municipal wastewater using new mode of dispersive liquid-liquid microextraction based on the solidified deep eutectic solvent followed by GFAAS, *Journal of the Science of Food and Agriculture*, *99*(2), 656-665.

Hintelmann, H., Harris, R., Heyes, A., Hurley, J.P., Kelly, C.A., Krabbenhoft, D.P., et al. (2002). Reactivity and mobility of new and old mercury deposition in a Boreal forest ecosystem during the first year of the METAALICUS study, *Environmental Science & Technology*, *36*(23), 5034-5040.

Hu, Y.N., Cheng, H.F., & Tao, S. (2016). The Challenges and Solutions for Cadmium-contaminated Rice in China: A Critical Review, *Environment International*, *92-93*, 515-532.

Huang, S., Rao, G., Ashraf, U., He, L., Zhang, Z., Zhang, H., et al. (2020). Application of inorganic passivators reduced Cd contents in brown rice in oilseed rape-rice rotation under Cd contaminated soil, *Chemosphere*, *259*.

Imseng, M., Wiggenhauser, M., Keller, A., Mueller, M., Rehkamper, M., Murphy, K., et al. (2018). Fate of Cd in Agricultural Soils: A Stable Isotope Approach to Anthropogenic Impact, Soil Formation, and Soil-Plant Cycling, *Environmental Science & Technology*, *52*(4), 1919-1928.

Javed, M.B., Cuss, C.W., Grant-Weaver, I., & Shotyk, W. (2017). Size-resolved Pb distribution in the Athabasca River shows snowmelt in the bituminous sands region an insignificant source of dissolved Pb, *Sci Rep*, *7*, 43622.

Jordi, A., Basterretxea, G., Tovar-Sanchez, A., Alastuey, A., & Querol, X. (2012). Copper aerosols inhibit phytoplankton growth in the Mediterranean Sea, *Proceedings of the National Academy of Sciences of the United States of America*, *109*(52), 21246-21249.

Larson, C. (2014). China Gets Serious About Its Pollutant-Laden Soil, *Science*, *343*(6178), 1415-1416.

Lee, P.K., Choi, B.Y., & Kang, M.J. (2015). Assessment of mobility and bio-availability of heavy metals in dry depositions of Asian dust and implications for environmental risk, *Chemosphere*, *119*, 1411-1421.

Li, F.L., Liu, C.Q., Yang, Y.G., Bi, X.Y., Liu, T.Z., & Zhao, Z.Q. (2012). Natural and anthropogenic lead in soils and vegetables around Guiyang city, southwest China: a Pb isotopic approach, *Science of the Total Environment*, *431*(5), 339-347.

Li, W., Wang, Y., Collett, J.L., Jr., Chen, J., Zhang, X., Wang, Z., et al. (2013). Microscopic evaluation of trace metals in cloud droplets in an acid precipitation region, *Environmental Science & Technology*, *47*(9), 4172-4180.

Liu, G., Meng, J., Huang, Y., Dai, Z., Tang, C., & Xu, J. (2020). Effects of carbide slag, lodestone and biochar on the immobilization, plant uptake and translocation of As and Cd in a contaminated paddy soil, *Environmental pollution (Barking, Essex : 1987)*, *266*(Pt 1), 115194-115194.

Liu, H., Li, M., Zhou, J., Zhou, D., & Wang, Y. (2017). Effects of soil properties and aging process on the acute toxicity of cadmium to earthworm Eisenia fetida, *Environmental Science & Pollution Research*.

Ma, X., Geiser-Lee, J., Deng, Y., & Kolmakov, A. (2010). Interactions between engineered nanoparticles (ENPs) and plants: Phytotoxicity, uptake and accumulation, *Science of the Total Environment*, *408*(16), 3053-3061.

Morselli, L., Olivieri, P., Brusori, B., & Passarini, F. (2003). Soluble and insoluble fractions of heavy metals in wet and dry atmospheric depositions in Bologna, Italy, *Environmental Pollution*, *124*(3), 457-469.

Peng, C., Chen, S., Shen, C., He, M., Zhang, Y., Ye, J., et al. (2018). Iron Plaque: A Barrier Layer to the Uptake and Translocation of Copper Oxide Nanoparticles by Rice Plants, *Environmental Science & Technology*, *52*(21), 12244-12254.

Peng, H., Chen, Y., Weng, L., Ma, J., Ma, Y., Li, Y., et al. (2019). Comparisons of heavy metal input inventory in agricultural soils in North and South China: A review, *Science of the Total Environment*, *660*, 776-786.

Prieto-Parra, L., Yohannessen, K., Brea, C., Vidal, D., Ubilla, C.A., & Ruiz-Rudolph, P. (2017). Air pollution, PM 2.5 composition, source factors, and respiratory symptoms in asthmatic and nonasthmatic children in Santiago, Chile, *Environment International*, *101*, 190-200.

Pyeong-Koo, L., Byoung-Young, C., & Min-Ju, K. (2015). Assessment of mobility and bio-availability of heavy metals in dry depositions of Asian dust and implications for environmental risk, *Chemosphere*, *119*, 1411-1421.

Salmanzadeh, M., Hartland, A., Stirling, C.H., Balks, M.R., Schipper, L.A., Joshi, C., et al. (2017). Isotope Tracing of Long-Term Cadmium Fluxes in an Agricultural Soil, *Environmental Science & Technology*, *51*(13), 7369-7377.

Schreck, E., Dappe, V., Sarret, G., Sobanska, S., Nowak, D., Nowak, J., et al. (2014). Foliar or root exposures to smelter particles: Consequences for lead compartmentalization and speciation in plant leaves, *Science of the Total Environment*, *476*, 667-676.

Shahid, M., Dumat, C., Khalid, S., Schreck, E., Xiong, T., & Niazi, N.K. (2016). Foliar heavy metal uptake, toxicity and detoxification in plants: A comparison of foliar and root metal uptake, *Journal of Hazardous Materials*, *325*, 36-58.

Stolpe, B., Guo, L., Shiller, A.M., & Aiken, G.R. (2013). Abundance, size distributions and trace-element binding of organic and iron-rich nanocolloids in Alaskan rivers, as revealed by field-flow fractionation and ICP-MS, *Geochimica et Cosmochimica Acta*, *105*, 221-239.

Tian, H.Z., Zhu, C.Y., Gao, J.J., Cheng, K., Hao, J.M., Wang, K., et al. (2015). Quantitative assessment of atmospheric emissions of toxic heavy metals from anthropogenic sources in China: historical trend, spatial distribution, uncertainties, and control policies, *Atmospheric Chemistry and Physics*, *15*(17), 10127-10147.

Uzu, G., Sobanska, S., Aliouane, Y., Pradere, P., & Dumat, C. (2009). Study of lead phytoavailability for atmospheric industrial micronic and sub-micronic particles in relation with lead speciation, *Environmental Pollution*, *157*(4), 1178-1185.

Wang, F.J., Chen, Y., Guo, Z.G., Gao, H.W., Mackey, K.R., Yao, X.H., et al. (2017). Combined effects of iron and copper from atmospheric dry deposition on ocean productivity, *Geophysical Research Letters*, *44*(5), 2546-2555.

Wang, P., Menzies, N.W., Chen, H., Yang, X., McGrath, S.P., Zhao, F., et al. (2018). Risk of Silver Transfer from Soil to the Food Chain Is Low after Long Term (20 Years) Field Applications of Sewage Sludge, *Environmental Science & Technology*, *52*(8), 4901-4909.

Werkenthin, M., Kluge, B., & Wessolek, G. (2014). Metals in European roadside soils and soil solution – A review, *Environmental Pollution*, *189*, 98-110.

Wilcke, W., & Kaupenjohann, M. (1998). Heavy metal distribution between soil aggregate core and surface fractions along gradients of deposition from the atmosphere, *Geoderma*, *83*(1-2), 55-66.

Zhang, H.X., Mao, Z.X., Huang, K., Wang, X., Cheng, L., Zeng, L.S., et al. (2019). Multiple exposure pathways and health risk assessment of heavy metal(loid)s for children living in fourth-tier cities in Hubei Province, *Environment International*, *129*, 517-524.

Zhao, F.J., Ma, Y.B., Zhu, Y.G., Tang, Z., & McGrath, S.P. (2015). Soil Contamination in China: Current Status and Mitigation Strategies, *Environmental Science & Technology*, *49*(2), 750-759.

Zhou, J., Liang, J., Hu, Y., Zhang, W., Liu, H., You, L., et al. (2018). Exposure risk of local residents to copper near the largest flash copper smelter in China, *Science of the Total Environment*, *630*, 453-461.

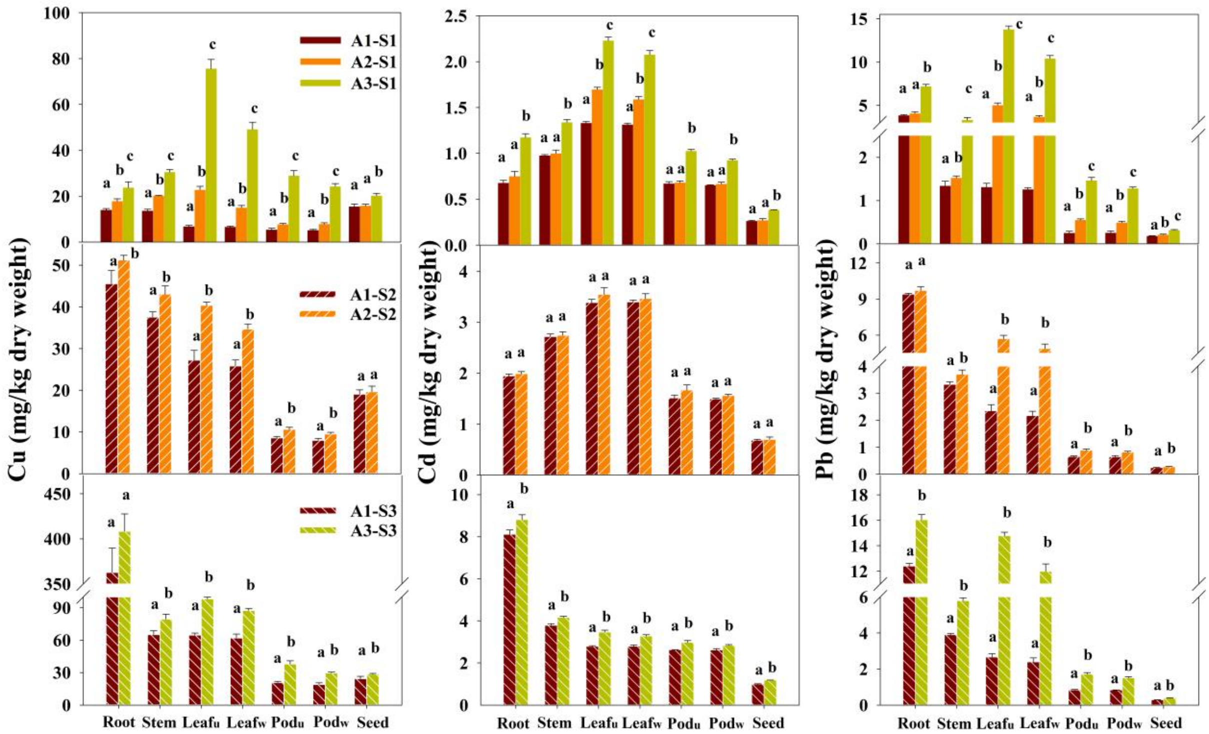

Fig. 1. Concentrations of Cu, Cd, and Pb in root, stem, leaf$_u$ (without washing), leaf$_w$ (washing), pod$_u$ (without washing), pod$_w$ (washing), and seed of soybean. Different letters indicate values significantly different among three deposition sites ($p < 0.05$).

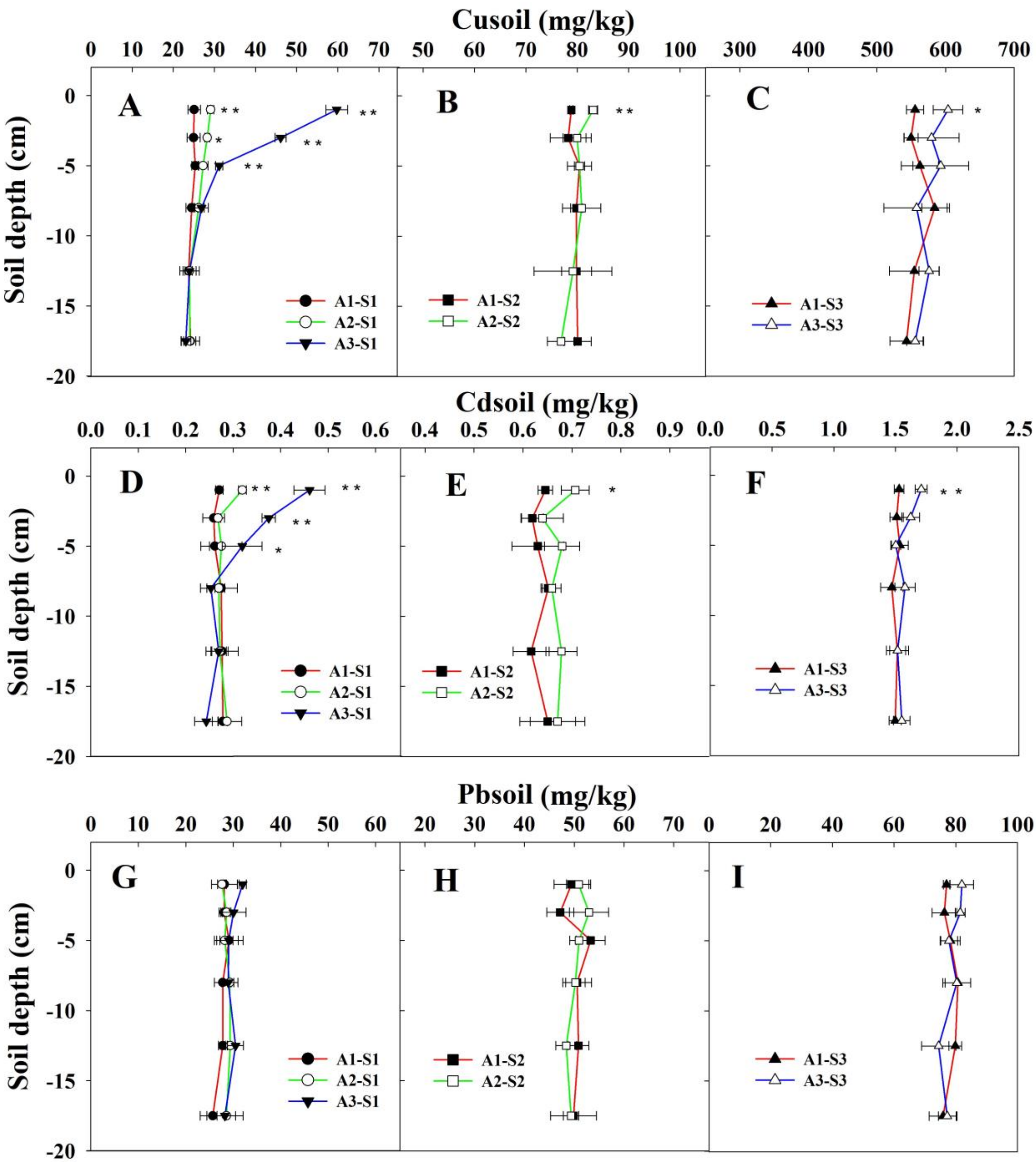

Fig. 2. Cu, Cd, and Pb concentrations in soils (0-20 cm profile). One asterisk and two asterisks indicate values significantly different between the deposition sites (A2 and A3) and control site (A1) ($p < 0.05$ and $p < 0.01$).

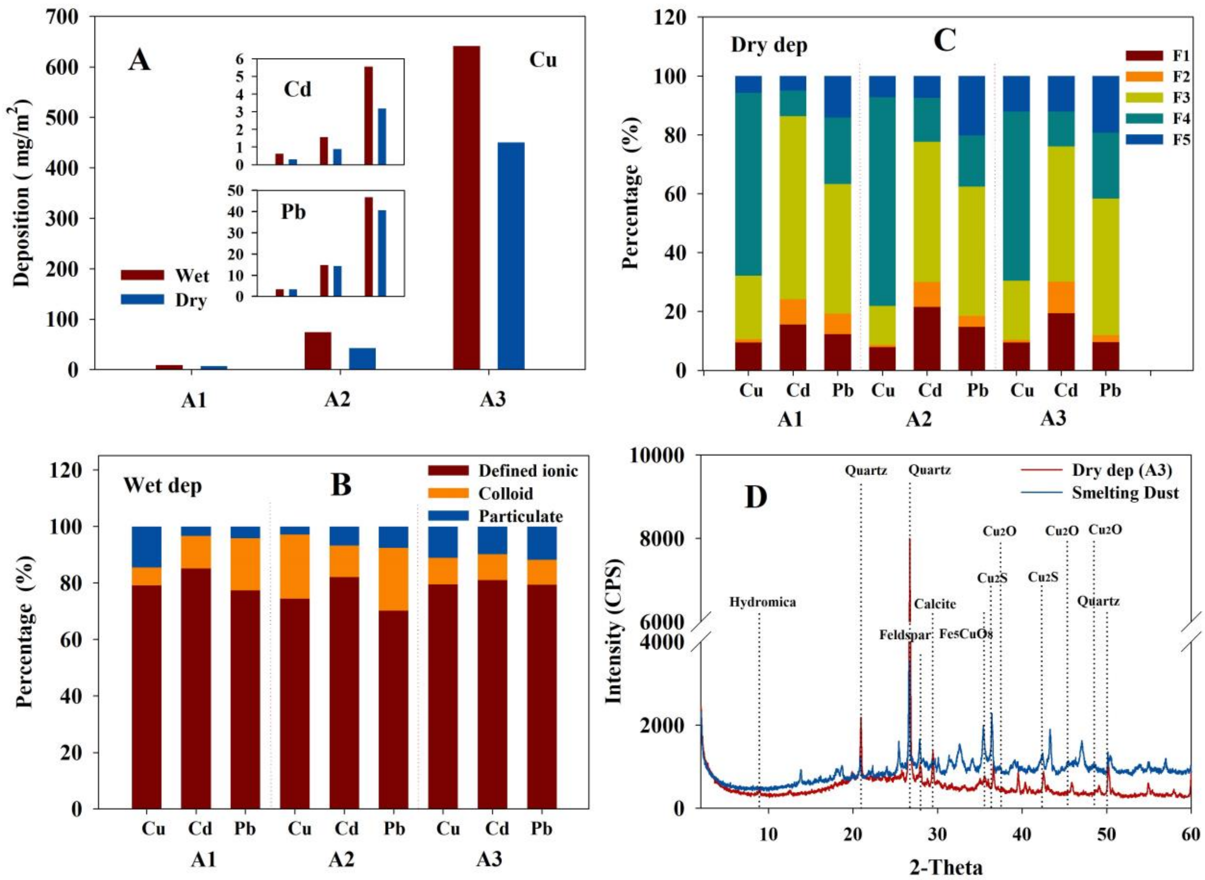

Fig. 3. Atmospheric wet and dry deposition flux (mg/m^2) of Cu, Cd, and Pb in July 2017 to June 2018 (A). The percentage of Cu, Cd, and Pb in size range of wet deposition and the chemical partitioning of dry deposition are given (B and C). The mineral composition of dry deposition and the dust from smelting are also given (D).

Supporting information of

Chemical speciation of trace metals in atmospheric deposition and impacts on soil geochemistry and vegetable bioaccumulation near a large copper smelter in China

Hai-Long Liu [a, b] Jun Zhou [a, c, d,] *, Min Li [b], Daniel Obrist [c], Xiao-Zhi Wang [b], Jing Zhou [a, d,] *

a. Key Laboratory of Soil Environment and Pollution Remediation, Institute of Soil Science, Chinese Academy of Sciences, Nanjing 210008, P.R. China

b. College of Environmental Science and Engineering, Yangzhou University, Yangzhou 225000, P.R. China

c. Department of Environmental, Earth and Atmospheric Sciences, University of Massachusetts, Lowell, MA 01854, USA

d. National Engineering and Technology Research Center for Red Soil Improvement, Red Soil Ecological Experiment Station, Chinese Academy of Sciences, Yingtan 335211, P.R. China

*Corresponding author: zhoujun@issas.ac.cn (Jun Zhou) and zhoujing@issas.ac.cn (Jing Zhou).

Add: 71st East Beijing Road, Nanjing, China, 210008.

Summary

25 SI pages containing 5 texts, 5 figures and 8 tables

Text S1

Study site

The study was conducted nearby the largest Cu smelter in China located in Guixi city of Jiangxi province in southeastern China (Supplementary information, Fig. S1). The climate is typical subtropical humid with an annually average temperature of 18 ^{o}C, average annual rainfall of 1905 mm and prevailing northeastern winds. The production capacity of the smelter was about 7.2×10^5 tons of Cu in 2018. Some other accessory products were also produced simultaneously, such as 1.65×10^5 tons of H_2SO_4, 1.4×10^3 tons of As_2O_3, 1.3×10 tons of gold (Au), and 3.5×10^2 tons of silver (Ag) per year (Xiao et al., 2011). Due to a large amount of metal smelting, the surrounding farmland has been heavily polluted, resulting in trace metals concentrations in crops exceeding the acceptable level (Xu et al., 2017a). Annual atmospheric deposition fluxes of trace metals around the smelter between July 2012 to June 2016 were 767.0 $mg\cdot m^{-2}\cdot a^{-1}$, 6.6 $mg\cdot m^{-2}\cdot a^{-1}$, and 70.0 $mg\cdot m^{-2}\cdot a^{-1}$ for Cu, Cd, and Pb, respectively (Zhou et al., 2018).

Three study sites (A1, A2, and A3) along an expected gradient of atmospheric deposition near the smelter were selected, including: a high atmospheric deposition site (A3) located about 1 km downwind from the smelter; a moderate atmospheric deposition site (A2) located about 6 km away following the same direction as site A3; and a control site with low deposition (A1) located about 34 km away, also following the same direction as sites A2 and A3 (Supplementary information, Fig. S1).

Text S2

Soil properties and measuring method

Soils properties used to grow vegetables were showed in Table S1. In short, soils (S1, S2, and S3) were hydragric anthrosols, acidic (pH_{CaCl_2}=4.3-5.3), and moderately fertile (OM=27-41 g/kg, CEC=7.4-8.8 cmol/kg), with available nitrogen of 113-185 mg/kg, available phosphorus of 34-58 mg/kg, and available potassium of 67-76 mg/kg). Soils S2 taken from the atmospheric exposure site A2 were moderately polluted (80.02±0.88 mg/kg Cu, 0.72±0.05 mg/kg Cd and 50.20±0.43 mg/kg Pb) while soils S3 from site A3 were heavily polluted (556.67±12.61 mg/kg Cu, 1.66±0.05 mg/kg Cd, and 74.13±1.77 mg/kg Pb) due to the long-term metal smelting emissions. Soil S1 from the control site (A1) was not or only minimally affected by smelting emissions (23.32±0.09 mg/kg Cu, 0.22±0.01 mg/kg Cd, and 29.61±0.19 mg/kg Pb) and lower than the regulatory limit for soil pollution of agricultural land by the China Ministry of Ecology and Environment (GB 15618-2018, 50 mg/kg for Cu, 0.3 mg/kg for Cd, and 70 mg/kg for Pb). While in general soil physicochemical properties of soils from the three study sites were similar (Table S1), soil pH and available P were higher in soils S3 due to previous applications of alkaline materials containing phosphorus to stabilize trace metals as a farmland remediation technique (Xu et al., 2017b).

Soil pH was measured in 0.01M $CaCl_2$ (1 : 2.5 soil : solution ratio). OM was measured by the Walkley and Black method (Potassium dichromate oxidation-ferrous sulphate titrimetry). Soil texture (percent sand, silt, and clay) was analyzed by Laser particle size analyzer (Beckman LS 13320, America). Cation exchange capacity (CEC) was measured by the ammonium acetate centrifugal exchange method. Available N was measured by the alkaline hydrolysis diffusion method. Available P was measured by Mo-Sb colorimetry. Available K was measured by ammonium acetate extraction-flame spectrophotometry. The values of trace metals in soils were determined by the inductively coupled plasma mass spectrometry (Agilent 7800 ICP-MS, America) with mixed-acid digestion (HNO_3-$HClO_4$-HF). Blanks and the certified soil reference material (GBW07406, the National Research Center for Standard Materials of China) were used for controlling the quality of our analysis and the recovery rates were 96-105%.

Text S3

Method of the fully factorial exposure experiment

In order to distinguish the recently trace metals by atmospheric deposition (<1 year) and the original trace metals (including parent rock matrix and earlier deposited atmospheric trace metals), a fully factorial soil and atmosphere exposure design with replications (n = 3) including seven treatment groups was conducted between July 2017 and June 2018. The polluted soils in moderate and high sites of atmospheric deposition were transferred to a control site and the unpolluted soil in control site was transferred to moderate and high deposition sites. In brief, the first treatment pot was a control site-box (A1-S1), located at A1 site, and filled with topsoil collected from A1 paddy field with the low levels of trace metals (23.32±0.09 mg/kg Cu, 0.22±0.01 mg/kg Cd, and 29.61±0.19 mg/kg Pb). This box received a comparatively low trace metals input by atmospheric deposition. The second treatment pot was also a control site-box (A1-S2), located at A1 site, but filled with A2 paddy field topsoil (S2) with the moderately polluted levels of trace metals (80.02±0.88 mg/kg Cu, 0.72±0.05 mg/kg Cd, and 50.20±0.43 mg/kg Pb). The third pot was a control site-box (A1-S3), located at A1 site, and filled with topsoil collected from A3 paddy field (S3) with the heavily polluted levels of trace metals (556.67±12.61 mg/kg Cu, 1.66±0.05 mg/kg Cd, and 74.13±1.77 mg/kg Pb). The pots of A1-S1, A1-S2 and A1-S3 received a low trace metals input by atmospheric deposition throughout the cultivation duration. The fourth pot was a moderate deposition site-box (A2-S1), located at A2 site receiving the moderate metals input by atmospheric deposition, but filled with the paddy field with the low levels of trace metals from A1 site. The fifth pot was also a moderate deposition site-box (A2-S2), located at A2 site receiving the same deposition input as A2-S1, and filled with the moderately polluted paddy soil from A2 site itself. The sixth pot was a high deposition site-box (A3-S1), located at A3 site, but filled with A1 paddy field topsoil with the low levels of trace metals. The box received a high trace metals input by atmospheric deposition. The seventh box was also a high deposition site-box (A3-S3), located at A3 site, and filled with the heavily polluted paddy soil from A3 site itself. To manage the high number of treatment numbers, we selected not to expose soil from moderate deposition site A2 at the high atmospheric deposition site A3, and vice versa not to expose soil from the high deposition site A3 at the moderate atmospheric deposition site A2. All boxes filled with soil profiles (dimensions: 0.58 m length×0.44 m wide×0.32 m height) were mounted on the stone mounds about 0.5 m above the surrounding ground in order to avoid any contamination from soil particles by splashing during heavy rainfall. These boxes were also filled with 10 mm thickness acid washed quartz and 40 mesh nylon mesh in the bottom with hole (3 cm in diameter) in order to discharge excess water in the rainy season.

Three wide cultivation vegetables in study area, including radish (*Raphanus sativus* L., rhizome vegetable), lettuce (*Lactuca sativa* L., leaf vegetable) and soybean (*Phaseolus vulgaris* L., fruit vegetable) were grown in each of these combined soil-atmosphere exposure categories, resulting in a total of 63 plant samples for the study (2-3 soil exposures, 3 atmospheric exposures, 3 vegetable types, 3 replications). The vegetable types were chosen because they represented different edible parts for human consumption, such as rhizomes for radish, leaves for lettuce and seeds for soybean. The planting order and growing season of the three vegetables were chosen according to local farming practices. Germinated radish seeds were firstly cultivated in the experimental with a density of 4 seedlings each pot in early January 2018. The radish was exposed for 60 d and then the lettuce seedlings (mean 8 g for fresh biomass, with the germinated seeds firstly cultivated in uncontaminated soils for one month) were continuously transplanted into plots in early March 2018. The lettuce was exposed for 45 d, after which the germinated soybean seeds were continuously transplanted into plots in mid-April 2018 and the mature soybean was harvested in late June 2018. Vegetables were watered by the qualified tap water containing the low concentrations of trace metals (Cu < 0.1 μg/L, Cd < 0.01 μg/L, and Pb < 0.01 μg/L) during the entire experiment. The effect of trace metals in the irrigation water was negligible compared with atmospheric deposition trace metals.

The objective of A1-S1 (filled with soil from the control site) exposed to low atmospheric deposition was to estimate bioaccumulation of trace metals in three vegetables from background soils (not/minimally affected by recent or earlier atmospheric deposition). Further, the key difference among A1-S3, A1-S2, and A1-S3 was the pollution level of trace metals in soils. The objective of three groups was to estimate bioaccumulation of trace metals in three vegetables from soils exposures, which would be indicative of the effect of past (i.e., >1 year) atmospheric deposition impacts (Zhou et al., 2018). Moreover, the key difference among A1-S1, A2-S1, and A3-S1 was the deposition flux. The objective of three groups was to understand whether the recently deposited trace metals are readily absorbed and accumulated in vegetable. Meanwhile, the objective of group A1-S2 and A2-S2 was to understand the process of trace metals accumulation from the moderately polluted soil and air. In addition, the objective of group A1-S3 and A3-S3 was to understand the contribution of trace metals accumulation in vegetable from the heavily polluted soil and air. The bioavailability of the recently deposited Cu, Cd, and Pb and those in original soil for vegetable can be well distinguished using such experimental design method. The bioaccumulation effect from the recently deposited trace metals on different edible types of vegetables also can be well investigated by this experiment.

Text S4

Method of sampling and analytical deposition

The atmospheric deposition samples during the period July 2017 to June 2018 were collected each month by automatic wet and dry deposition sampler (APS-3A, Changsha Xianglan Scientific Instruments Co., Hunan, China) situated on the rooftops of buildings at each site to minimize local soil contamination. The collector was equipped with one moisture sensor to collect dry and wet deposition separately. The moisture sensor would activate the electric pathway allowing automatic transfer of the dustproof cover from wet deposition polyethylene bottle to dry deposition polyethylene bottle during the rain event. The sampler was washed every month by 2% HNO_3 solution and 0.2% benzalkonium chloride (Osvan) for sterilization (Osada et al., 2014). For wet deposition, the sample was not collected in October 2017 due to absent rain; for dry deposition each month, a plastic brush was carefully used to collect deposition particles, and then they were stored in polypropylene centrifuge tube at 4 ^{o}C (Corning, USA) and brought into laboratory for subsequent analyses. The operating principle of collector in detail can be obtained from the previous study (Wang et al., 2012).

In wet deposition, the rain samples of each month were divided into two equal parts, and one was used to determine pH and hydrodynamic diameter by Dynamic light scattering (DLS, NanoBrook 90Plus PALS, America). The other part was used to measure size distribution of Cu, Cd, and Pb, whereby size distribution included separation into particulate (> 0.45 μm, unfiltered samples), dissolved (corresponding colloid fraction, < 0.45 μm, filtered by 0.45 μm filter) (PES, MEMBRANA, Germany), and defined ionic fraction (i.e., ionic metals and those adsorbed onto small molecular weight colloid, < 3 kDa, filtered by 3 kDa filter) (Amicon Ultra-15, Millipore, USA) (Javed et al., 2017). All rain samples analyzed for species of trace metals (Cu, Cd, and Pb) were extracted using nitric acid (5%, *v/v*) facilitated by heating under 80 ℃ according to the modified method of USEPA 200.8 and determined by ICP-MS (Agilent 7800, America) (Wang et al., 2017).

For dry deposition, samples were air-dried, grinded and sieved to < 0.15 mm. One of the halves samples each month were used to conduct the characterization of mineral composition by X-ray diffractometer XRD (Ultima IV, Japan) analysis. Dust samples from pulse bag filter from the Guixi copper smelter were also collected and sieved to < 0.15 mm to assist in the characterization of trace metal hosting mineral phases by XRD considering that the low trace metal content in atmospheric deposition cannot meet the

XRD identification limit, which can be also used for verifying the likely origin of atmospheric deposition and links to this assumed emission source. The other halves were used to conduct Tessier five-step sequential extraction (F1 exchangeable, F2 carbonate, F3 reducible, F4 organic and sulfide, and F5 residual fractions) determining the partitioning of trace metals (Cu, Cd, and Pb) by ICP-MS (Agilent 7800, America) (Lee et al., 2015). Blanks and the certified soil reference material (GBW07442, the National Research Center for Standard Materials of China) were used for controlling the quality of our analysis and the recovery rates were 97-103%. These characteristics were conducive to analyze the mobility and bioavailability of atmospheric deposition trace metals.

Text S5

Method of sampling and analytical vegetable and soil

The three vegetables (radish, lettuce, and soybean) grown in sequence for the duration of 60, 45, and 75 days, respectively were harvested in early March, mid-April, and late June 2018, respectively. Sampling radish and lettuce were dissected into shoot and rhizome (or root) washed by running tap water and then deionized water (Uzu et al., 2010), and the root, stem, and seed of soybean were also washed by the same operation as above. Additionally, the leaf and pod (excluding seed) of soybean were both splitted in two sub samples and one was washed as above and the other halve was unwashed and cleaned carefully with a brush to compare and study the effect of the direct foliar absorption of atmospheric deposition pollutants on trace metals accumulation in vegetables (De Temmerman et al., 2015). The fresh weight and dry weight of vegetable tissues were weighed separately, and then samples were dried at 105 ℃ for 30 min and 80 ℃ to a constant weight, grinded, sieved to < 0.15 mm and Cu, Cd, and Pb of vegetable samples were extracted in a 1:1 mixture of HNO_3 and H_2O_2 at 90 ℃ for 4 h. Meanwhile, the corresponding surface soils after harvest of the soybean in late June 2018 were collected by stratified sampling (0-2, 2-4, 4-6, 6-10, 10-15, and 15-20 cm, three samples constituting one pooled sample per layer per pot) and stored in liquid nitrogen. Tessier five-step sequential extraction (F1 exchangeable, F2 carbonate, F3 reducible, F4 organic and sulfide, and F5 residual fractions) was performed using 1.0 g sub-samples of soils within polypropylene centrifuge tubes to determine the partitioning of Cu, Cd, and Pb in soils.

Soil and plant extracted samples were determined by ICP-MS (Agilent 7800, America) for Cu, Cd, and Pb. Blanks and the certified soil and spinach reference material (GBW07442 and 10015, the National Research Center for Standard Materials of China) were used for controlling the quality of our analysis and the recovery rates were 96-102%.

Table S1

Soil properties of all three study sites. Data are shown as mean ± SD (n = 3).

Soil ID	S1	S2	S3
Soil type	Hydragric anthrosols	Hydragric anthrosols	Hydragric anthrosols
Latitude	116°56′20″ E	117°10′8″ E	117°12′32″ E
Longitude	28°12′29″ N	28°17′42″ N	28°19′44″ N
pH	4.28±0.03	4.45±0.01	5.27±0.02
OM (g/kg)	40.62±0.91	27.13±0.62	32.05±0.81
CEC (cmol/kg)	8.81±0.01	8.32±0.08	7.35±0.03
Clay %	27.45±0.07	22.80±0.14	15.50±0.09
Silt %	48.35±0.21	40.7±0.01	23.70±0.14
Sand %	23.60±0.12	36.13±0.08	57.15±0.23
Available N (mg/kg)	184.69±1.59	146.81±1.79	113.41±2.85
Available P (mg/kg)	34.11±0.58	43.55±1.02	58.09±0.26
Available K (mg/kg)	74.10±2.40	67.18±0.88	75.75±2.33
Cd (mg/kg)	0.22±0.01	0.72±0.05	1.66±0.05
Cu (mg/kg)	23.32±0.09	80.02±0.88	556.67±12.61
As (mg/kg)	5.58±0.13	11.24±0.42	50.17±0.59
Pb (mg/kg)	29.61±0.19	50.20±0.43	74.13±1.77
Cr (mg/kg)	63.76±0.85	52.45±0.70	38.28±1.11
Zn (mg/kg)	52.41±0.48	80.27±0.68	77.55±2.15
Ni (mg/kg)	16.53±0.23	16.07±0.23	12.78±0.40

Table S2

Descriptive design of a fully factorial soil and atmosphere exposure experiment including seven treatment groups.

Soil substrate/Atmospheric exposure	A1: Low atmospheric deposition (control)	A2: Moderate atmospheric deposition	A3: High atmospheric deposition
S1: Background soil (control)	A1-S1	A2-S1	A3-S1
S2: Moderate soil pollution	A1-S2	A2-S2	---
S3: Heavy soil pollution	A1-S3	---	A3-S3

Table S3

The contribution range (%) of recently atmospheric deposition to Cu, Cd, and Pb of soybean tissues.

Group	Cu					Cd					Pb				
	root	stem	leaf	pod	seed	root	stem	leaf	pod	seed	root	stem	leaf	pod	seed
A2-S1	21.6	32.6	56.8	35.1	2.6	9.5	2.3	17.3	2.2	3.2	5.5	12.2	65.7	47.7	14.2
A2-S2	11.1	12.8	25.6	15.9	3.0	2.4	1.0	2.0	4.4	2.2	3.3	10.2	55.7	21.0	11.3
A3-S1	41.2	55.4	86.8	78.9	23.8	42.2	27.1	36.7	29.4	31.3	46.5	59.7	87.9	79.9	42.4
A3-S3	11.2	18.1	29.1	35.6	14.6	8.0	9.2	15.0	8.0	15.8	22.7	32.6	80.1	44.8	27.3

Table S4

The contribution range (%) of recently atmospheric deposition to Cu, Cd, and Pb of radish tissues.

Group	Cu		Cd		Pb	
	rhizome	shoot	rhizome	shoot	rhizome	shoot
A2-S1	8.6	37.2	12.1	29.1	5.8	35.1
A2-S2	4.7	14.6	2.5	8.2	8.0	21.9
A3-S1	46.1	78.8	56.6	57.2	54.8	67.4
A3-S3	16.2	29.1	31.5	27.3	39.3	53.8

Table S5

The contribution range (%) of recently atmospheric deposition to Cu, Cd, and Pb of lettuce tissues.

Group	Cu		Cd		Pb	
	root	shoot	root	shoot	root	shoot
A2-S1	8.5	30.1	9.2	35.4	10.2	25.2
A2-S2	5.0	20.2	0.3	13.4	2.2	18.0
A3-S1	54.2	76.0	22.3	58.4	37.5	63.6
A3-S3	23.7	48.6	13.8	32.6	28.7	44.5

Table S6

The contribution range (%) of trace metals originally present in soils to vegetable bioaccumulation.

Vegetable	Soil substrate	Cu	Cd	Pb
soybean	moderate pollution S2	19.2	61.8	28.0
	heavy pollution S3	36.7	73.7	37.9
radish	moderate pollution S2	66.0	60.6	47.5
	heavy pollution S3	80.3	67.4	64.8
lettuce	moderate pollution S2	48.3	74.3	51.3
	heavy pollution S3	68.6	81.5	57.4

Table S7 The partitioning (F1 exchangeable, F2 carbonate, F3 reducible, F4 organic and sulfide, and F5 residual fractions) of Cu, Cd, and Pb (mg/kg) in soils (0-2 and 2-4 cm profile) exposed to atmospheric deposition over one year. Data are shown as mean ± SD (n = 3).

Metal	Group	F1		F2		F3		F4		F5	
		0-2cm	2-4 cm	0-2 cm	2-4 cm	0-2 cm	2-4 cm	0-2 cm	2-4 cm	0-2 cm	2-4 cm
Cu	A1-S1	1.5±0.1 ^{a}	1.6±0.1 ^{a}	0.5±0.0 ^{a}	0.5±0.0 ^{a}	1.5±0.1 ^{a}	1.4±0.1 ^{a}	13.1±0.2 ^{a}	12.7±0.8 ^{a}	8.1±0.5 ^{a}	7.9±0.4 ^{a}
	A2-S1	2.4±0.2 ^{b}	2.3±0.1 ^{b}	1.0±0.1^{b}	0.9±0.1^{b}	1.9±0.1^{b}	1.8±0.1^{b}	15.1±0.7 ^{b}	14.3±1.0 ^{a}	8.3±0.5 ^{a}	8.1±0.5 ^{a}
	A3-S1	9.2±0.3^{c}	5.7±0.2 ^{c}	5.0±0.1^{c}	2.9±0.0 ^{c}	5.1±0.1 ^{c}	4.2±0.2 ^{c}	25.7±1.5 ^{c}	21.2±1.1^{c}	10.2±0.5 ^{b}	9.3±0.4 ^{a}
	A1-S2	7.0±0.2 ^{a}	5.1±0.2 ^{a}	2.1±0.1 ^{a}	1.9±0.1 ^{a}	5.2±0.2 ^{a}	5.2±0.2 ^{a}	40±2 ^{a}	38±2 ^{a}	24±2 ^{a}	24±3 ^{a}
	A2-S2	8.5±0.3 ^{b}	5.1±0.3 ^{b}	2.4±0.2 ^{a}	2.0±0.1 ^{a}	5.6±0.3 ^{a}	5.3±0.2 ^{a}	41±3 ^{a}	40±3 ^{a}	24±1 ^{a}	23±2 ^{a}
	A1-S3	83±3 ^{a}	87±6 ^{a}	20±1 ^{a}	18±1 ^{a}	140±12 ^{a}	141±11 ^{a}	238±12 ^{a}	235±9 ^{a}	57±5 ^{a}	55±6 ^{a}
	A3-S3	93±4 ^{b}	92±7 ^{a}	23±1 ^{a}	19±1 ^{a}	150±13 ^{a}	147±16 ^{a}	255±15 ^{a}	248±5 ^{a}	60±8 ^{a}	58±7 ^{a}
Cd	A1-S1	0.06±0.00 ^{a}	0.06±0.00 ^{a}	0.07±0.00 ^{a}	0.07±0.00 ^{a}	0.07±0.00 ^{a}	0.07±0.00 ^{a}	0.06±0.00 ^{a}	0.05±0.00 ^{a}	0.05±0.00 ^{a}	0.05±0.00 ^{a}
	A2-S1	0.08±0.00 ^{b}	0.06±0.00 ^{a}	0.08±0.01 ^{a}	0.07±0.00 ^{a}	0.07±0.00 ^{a}	0.07±0.00 ^{a}	0.06±0.00 ^{a}	0.05±0.00 ^{a}	0.05±0.00 ^{a}	0.05±0.00 ^{a}
	A3-S1	0.13±0.01 ^{b}	0.09±0.00 ^{b}	0.09±0.00 ^{b}	0.08±0.00 ^{a}	0.09±0.01^{b}	0.07±0.00 ^{a}	0.08±0.01 ^{a}	0.07±0.01 ^{b}	0.06±0.00 ^{b}	0.05±0.00 ^{a}
	A1-S2	0.20±0.01 ^{a}	0.19±0.01 ^{a}	0.09±0.01 ^{a}	0.09±0.01 ^{a}	0.11±0.00 ^{a}	0.11±0.00 ^{a}	0.14±0.00 ^{a}	0.14±0.01 ^{a}	0.10±0.01 ^{a}	0.10±0.01 ^{a}
	A2-S2	0.25±0.01 ^{b}	0.20±0.01 ^{a}	0.10±0.01 ^{a}	0.09±0.01 ^{a}	0.12±0.01 ^{a}	0.11±0.00 ^{a}	0.15±0.01 ^{a}	0.14±0.00 ^{a}	0.10±0.00 ^{a}	0.11±0.01 ^{a}
	A1-S3	0.64±0.03^{a}	0.60±0.02 ^{a}	0.17±0.02 ^{a}	0.16±0.01 ^{a}	0.27±0.02 ^{a}	0.27±0.03 ^{a}	0.51±0.02 ^{a}	0.51±0.02 ^{a}	0.432±0.03 ^{a}	0.43±0.02 ^{a}
	A3-S3	0.73±0.02 ^{b}	0.65±0.03 ^{a}	0.22±0.03^{a}	0.20±0.02 ^{a}	0.30±0.03 ^{a}	0.28±0.02 ^{a}	0.54±0.03 ^{a}	0.51±0.02 ^{a}	0.43±0.04 ^{a}	0.43±0.05 ^{a}
Pb	A1-S1	1.02±0.05 ^{a}	1.03±0.07 ^{a}	1.45±0.09 ^{a}	1.34±0.10 ^{a}	6.44±0.19 ^{a}	6.38±0.20 ^{a}	7.20±0.13 ^{a}	7.43±0.15 ^{a}	18.7±0.7 ^{a}	18.6±0.9 ^{a}
	A2-S1	1.04±0.02 ^{a}	1.03±0.07 ^{a}	1.45±0.05 ^{a}	1.33±0.10 a	6.38±0.10 ^{a}	6.41±0.22 ^{a}	7.20±0.30 ^{a}	7.40±0.42 ^{a}	18.6±0.8 ^{a}	18.6±1.4 ^{a}
	A3-S1	1.20±0.15 ^{a}	1.14±0.12 ^{a}	1.46±0.20 ^{a}	1.37±0.15 ^{a}	6.83±0.24 ^{a}	6.77±0.30 ^{a}	7.21±0.21 ^{a}	7.93±0.61 ^{a}	18.4±1.1 ^{a}	18.8±0.8 ^{a}
	A1-S2	3.08±0.20 ^{a}	2.88±0.10 ^{a}	2.04±0.10 ^{a}	2.02±0.10 a	13.5±2.3 ^{a}	12.0±1.3 ^{a}	9.20±0.13 ^{a}	9.08±0.33 ^{a}	22.2±1.7 ^{a}	21.2±2.7 ^{a}
	A2-S2	3.15±0.31 ^{a}	2.95±0.20 ^{a}	2.14±0.10 ^{a}	2.07±0.10 a	14.0±1.8 ^{a}	12.1±2.5 ^{a}	9.30±0.32 ^{a}	9.14±0.42 ^{a}	22.8±2.1 ^{a}	22.0±1.5 ^{a}
	A1-S3	4.81±0.42 ^{a}	4.58±0.17 ^{a}	5.48±0.55 ^{a}	5.55±0.53 ^{a}	21.5±2.3 ^{a}	22.4±0.8 ^{a}	12.5±0.9 ^{a}	12.5±0.4 ^{a}	29.8±2.7 ^{a}	29.5±1.6 ^{a}
	A3-S3	4.95±0.72 ^{a}	4.89±0.37 ^{a}	6.35±0.90 ^{a}	6.23±0.56 ^{a}	21.7±1.3 ^{a}	22.9±1.7 ^{a}	12.7±0.4 ^{a}	11.8±0.8 ^{a}	30.7±2.1 ^{a}	29.6±1.7 ^{a}

Table S8

Hydrodynamic diameter distributions of fine particles (intensity) and pH in wet deposition over one year (July 2017 to June 2018). The precipitation is absent in October 2017. Data are shown as mean ± SD (n = 6).

Month	A1			A2			A3		
	Size (nm)	PDI*	pH	Size (nm)	PDI*	pH	Size (nm)	PDI*	pH
17-07	3.19±0.16	0.26±0.05	5.21±0.04	13.56±4.06	0.34±0.02	4.46±0.05	5.30±1.06	0.29±0.06	3.41±0.04
17-08	10.23±2.75	0.38±0.04	4.86±0.06	37.73±7.50	0.36±0.01	4.35±0.04	39.50±5.82	0.32±0.01	3.53±0.05
17-09	3.85±0.18	0.46±0.11	4.73±0.05	52.93±2.37	0.30±0.01	4.44±0.02	26.77±4.03	0.26±0.04	3.79±0.03
17-10	---	---	---	---	---	---	---	---	---
17-11	79.05±7.73	0.47±0.06	6.11±0.05	2.80±0.20	0.52±0.02	4.99±0.04	12.26±2.05	0.35±0.03	3.07±0.05
17-12	2.99±1.05	0.47±0.05	5.34±0.03	3.08±1.09	0.37±0.02	4.64±0.03	6.06±0.47	0.50±0.04	4.50±0.04
18-01	3.82±0.19	0.48±0.03	6.30±0.04	31.3±4.7	0.35±0.05	4.39±0.03	88.07±8.80	0.33±0.03	3.77±0.05
18-02	9.56±0.25	0.31±0.01	5.94±0.02	18.49±2.13	0.40±0.03	4.56±0.02	8.48±1.05	0.46±0.05	3.43±0.04
18-03	22.06±3.74	0.53±0.05	6.12±0.03	30.94±5.19	0.36±0.05	4.63±0.04	15.07±2.10	0.32±0.08	3.24±0.02
18-04	15.35±0.96	0.38±0.02	5.53±0.04	10.69±3.03	0.29±0.02	4.32±0.03	21.09±4.11	0.44±0.03	3.09±0.03
18-05	9.84±0.62	0.22±0.02	4.98±0.03	7.74±1.08	0.41±0.03	4.52±0.05	12.82±2.18	0.26±0.05	3.51±0.02
18-06	19.41±1.14	0.32±0.03	5.13±0.02	11.01±2.08	0.27±0.02	4.43±0.02	4.19±0.86	0.30±0.06	3.63±0.05

* PDI (particle dispersion index).

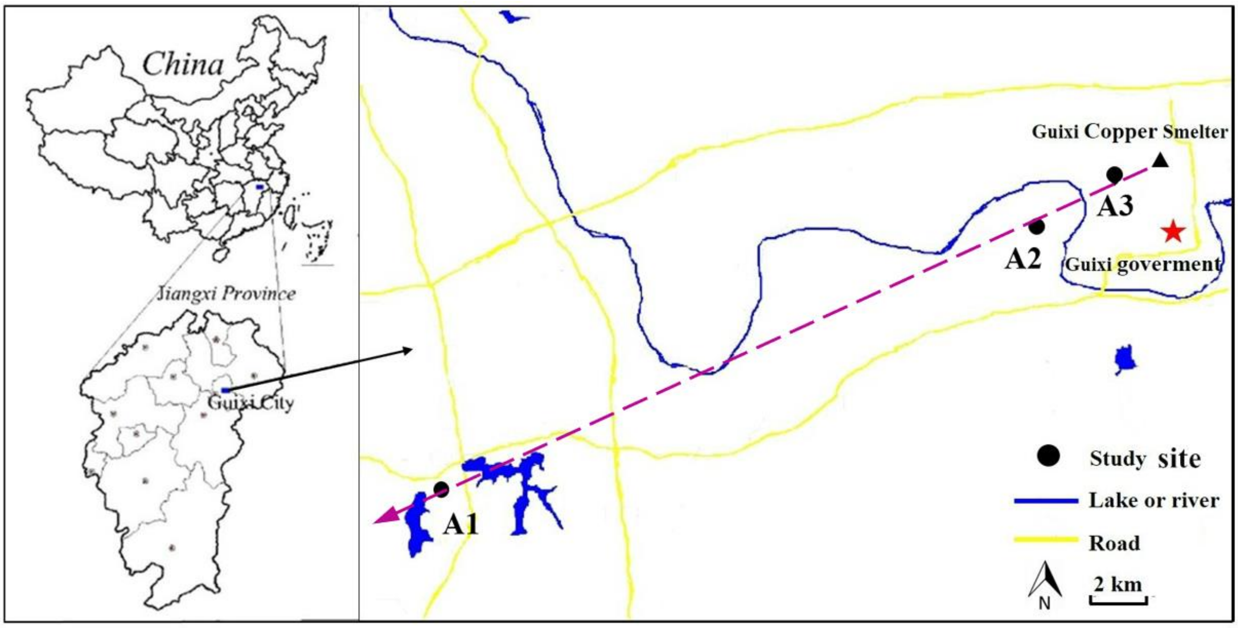

Fig. S1. Locations of the study sites.

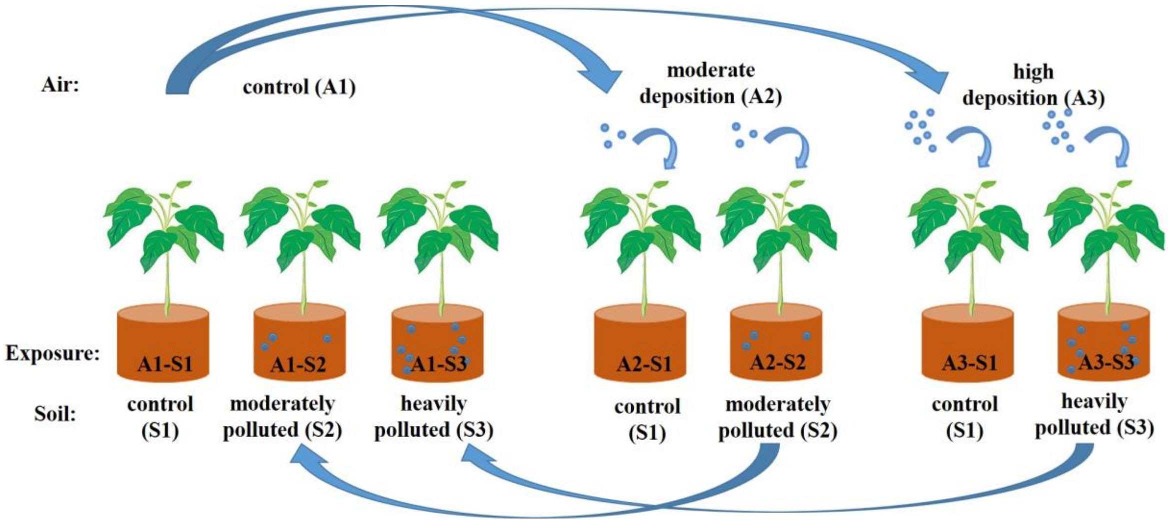

Fig. S2. Design of a fully factorial soil and atmospheric exposure experiment with vegetable including seven treatment groups.

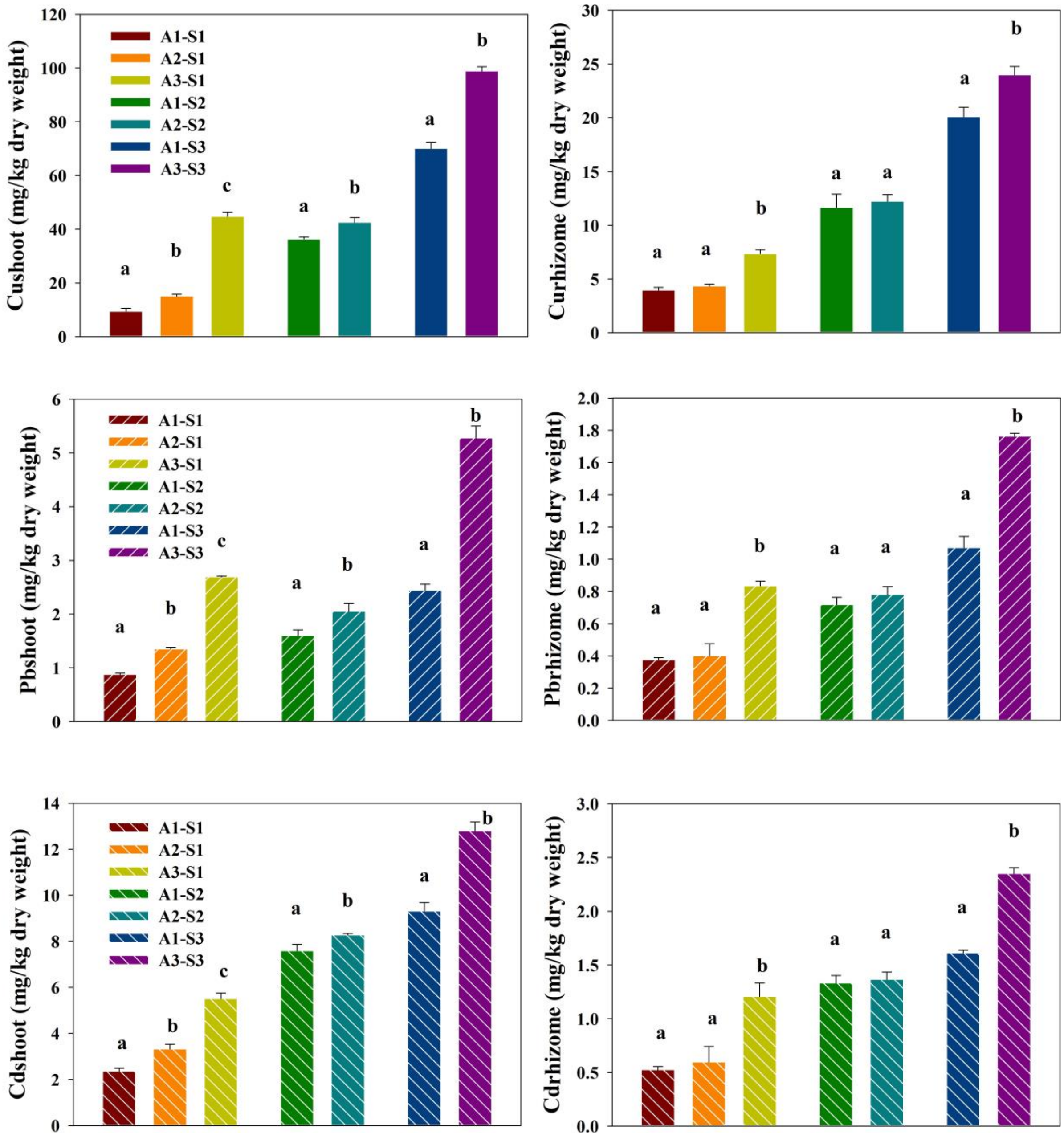

Fig. S3. Total Cu, Pb, and Cd concentrations of radish shoots and rhizomes collected from seven experiment groups in three study sites. Different letters indicate values significantly different among three deposition sites ($p < 0.05$). Data are shown as mean ± SD (n = 3).

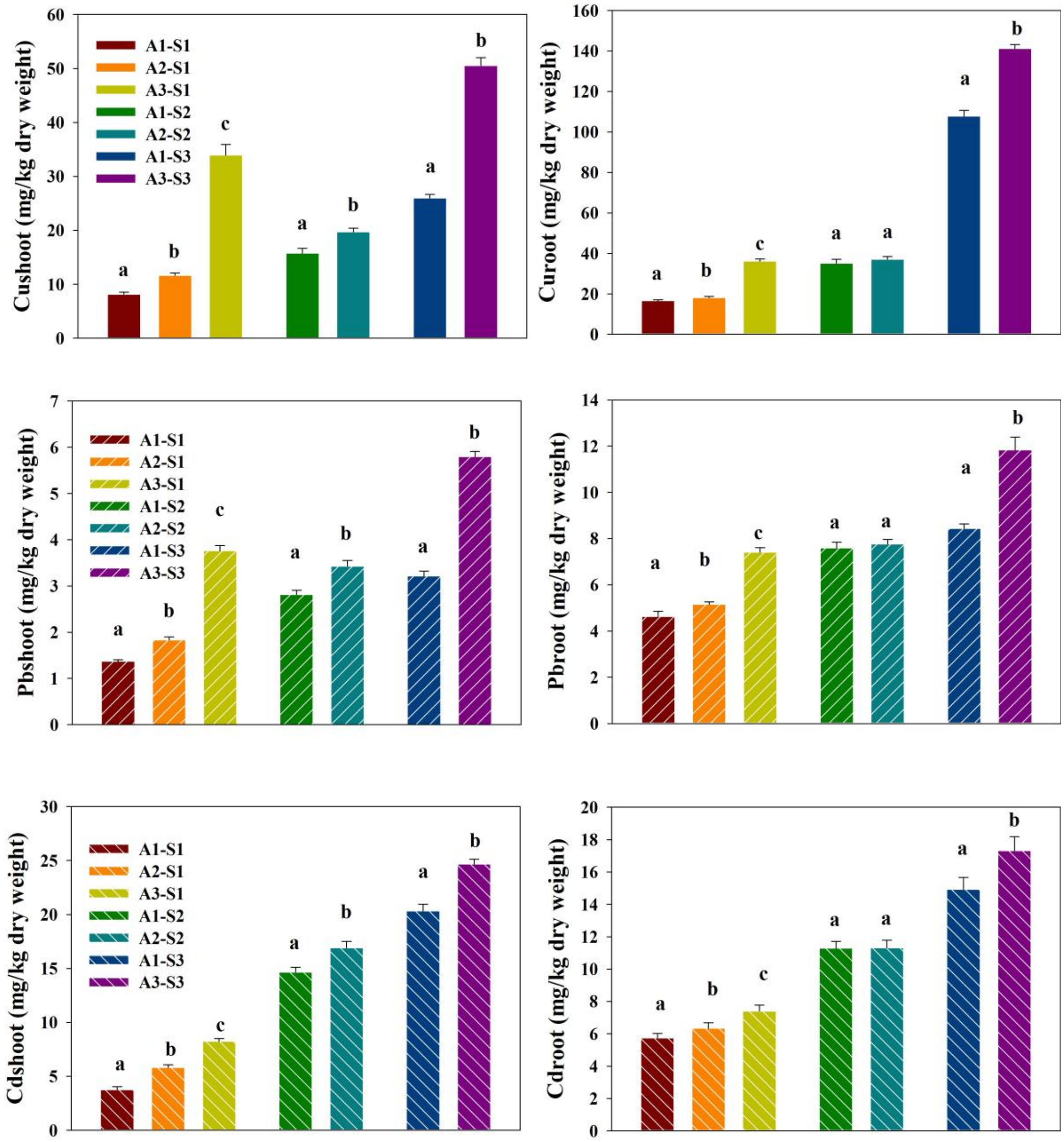

Fig. S4. Total Cu, Pb, and Cd concentrations of lettuce shoots and roots collected from seven experiment groups in three study sites. Different letters indicate values significantly different among three deposition sites ($p < 0.05$). Data are shown as mean ± SD (n = 3).

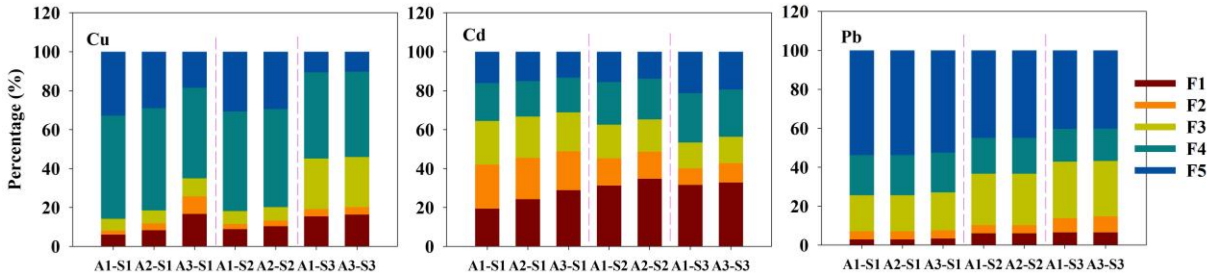

Fig. S5. The percentage of Cu, Cd, and Pb in soils (0-2 cm profile) exposed to atmospheric deposition over one year. Data are shown as mean (n = 3).

References

De Temmerman, L., Waegeneers, N., Ruttens, A., & Vandermeiren, K. (2015). Accumulation of atmospheric deposition of As, Cd and Pb by bush bean plants, *Environmental Pollution*, *199*, 83-88.

Javed, M.B., Cuss, C.W., Grant-Weaver, I., & Shotyk, W. (2017). Size-resolved Pb distribution in the Athabasca River shows snowmelt in the bituminous sands region an insignificant source of dissolved Pb, *Scientific Reports*, *7*, 1-11.

Lee, P.K., Choi, B.Y., & Kang, M.J. (2015). Assessment of mobility and bio-availability of heavy metals in dry depositions of Asian dust and implications for environmental risk, *Chemosphere*, *119*, 1411-1421.

Osada, K., Ura, S., Kagawa, M., Mikami, M., Tanaka, T.Y., Matoba, S., et al. (2014). Wet and dry deposition of mineral dust particles in Japan: factors related to temporal variation and spatial distribution, *Atmospheric Chemistry and Physics*, *14*(2), 1107-1121.

Uzu, G., Sobanska, S., Sarret, G., Munoz, M., & Dumat, C. (2010). Foliar lead uptake by lettuce exposed to atmospheric fallouts, *Environmental Science & Technology*, *44*(3), 1036-1042.

Wang, W., Chen, M., Guo, L., & Wang, W.X. (2017). Size partitioning and mixing behavior of trace metals and dissolved organic matter in a South China estuary, *Science of the Total Environment*, *603-604*, 434-444.

Wang, Y.M., Wang, D.Y., Meng, B., Peng, Y.L., Zhao, L., & Zhu, J.S. (2012). Spatial and temporal distributions of total and methyl mercury in precipitation in core urban areas, Chongqing, China, *Atmospheric Chemistry and Physics*, *12*(20), 9417-9426.

Xiao, H.-Y., Jiang, S.-Y., Wu, D.-S., & Zhou, W.-B. (2011). Risk element (as, cd, cu, pb, and zn) contamination of soils and edible vegetables in the vicinity of Guixi smelter, South China, *Soil and Sediment Contamination: An International Journal*, *20*(5), 592-604.

Xu, L., Cui, H., Zheng, X., Zhou, J., Zhang, W., Liang, J., et al. (2017a). Changes in the heavy metal distributions in whole soil and aggregates affected by the application of alkaline materials and phytoremediation, *RSC Advances*, *7*(65), 41033-41042.

Xu, L., Cui, H., Zheng, X., Zhou, J., Zhang, W., Liang, J., et al. (2017b). Changes in the heavy metal distributions in whole soil and aggregates affected by the application of alkaline materials and phytoremediation, *RSC. Adv.*, *7*(65), 41033-41042.

Zhou, J., Liang, J., Hu, Y., Zhang, W., Liu, H., You, L., et al. (2018). Exposure risk of local residents to copper near the largest flash copper smelter in China, *Science of the Total Environment*, *630*, 453-461.